

Corrosion Protection Enhancement on Aluminum Alloy And Magnesium Alloy by Mo-CeO₂ conversion coating

A. Ziouche^{(a)*}, A. Hammouda^(a), N. Boucherou^(a), M. Mokhtari^(b), B. Hafez^(c), H. Elmsellem^(d), S. Abaidia^(e).

^(a) Research Center in Industrial Technologies (CRTI), P.O. Box 64, Cheraga, 16014 Algiers, Algeria

^(b) Laboratory of valorization and technology of saharian resources (VTRS), faculty of technology, Hamma Lakhdar University, 39000, Algeria

^(c) Department of Pharmaceutical Sciences, College of Pharmacy and Health Sciences, Ajman University, Ajman, United Arab Emirates

^(d) LC2AME, Department of Chemistry, Faculty of Sciences, Mohamed 1st University, P.O. Box 717, Oujda 60000, Morocco

^(e) Department of Physics, ER-MPE, Boumerdes University, 35000, Algeria.

Abstract

In this paper, Mo-CeO₂ conversion coating developed to protect Aluminum 2024 alloy and Magnesium AZ31 alloy against corrosion. The cerium oxide incorporated in Molybdenum conversion coating, which considered as a promising alternative to replace chromate compounds. The corrosion efficacy was improving and characterized by polarization curves and EIS measurements. The structural and the microstructural Mo-CeO₂ conversion coating was characterized by AFM, SEM and XRD and the mechanical proprieties was determined by Nano indentation. The presence of molybdenum and oxide of cerium confirmed with good physical and mechanical proprieties. The presence of CeO₂ in the conversion coating had a beneficial effect on the corrosion resistance of the both materials.

* Corresponding author:

aicha_ziouche@yahoo.fr

Received 25 August 2021,

Revised 20 sept 2021,

Accepted 27 sept 2021,

Keywords: aluminum and magnesium alloys, Mo conversion coating, Nano coating CeO₂, Corrosion, EIS, AFM.

1. Introduction

Aluminum and magnesium alloys are widely used in the aeronautics field for its good physical and mechanical properties [1,2]. The corrosion resistance in confined or severe environments is reduced in aluminum and magnesium alloys. The presence of different kind of corrosion in industrials field reduce the performance and security of execution of the operation [3, 4]. In the past years, Cr(VI) based pre-treatments have been currently used for corrosion protection of different metals, however, they are toxic [3, 5]. Some alternatives to replace Cr(VI) show advantages key properties such as: corrosion resistance, durability and reliability [5-7]. However, some of their possible alternatives show high potential such as the conversion coating [7, 8-10]. In basic the conversion coatings using chromium compounds, which is toxic and carcinogenic nature. Therefore, alternative, conversion coatings based on molybdate are commonly used for this purpose, that are more environmentally-compliant [11-14]. The coatings prepared via conversion route show interesting properties in the field of the mechanics and more generally towards the anti-corrosive protection of metal substrates [4]. The conversion coating process including molybdenum ameliorate the surface properties protection correlated to the feasibility of efficient protection via a new eco-friendly route [3-6, 15-18]. Owing to its excellent corrosion protection performance, high adhesion strengths for their use as a coating material on a substrate, and also as being a promising environmentally friendly material, the cerium oxide coating has been extensively studied in recent decades and conversion coatings are an interesting category among them to be utilized to provide a surface modification for good corrosion protection of lightweight materials such as Al and Mg alloys [19-22]. In this paper, we present the incorporation of cerium oxide in molybdenum conversion coating, to study the behavior of the coating obtained applied on aluminum and magnesium alloy.

2. Materials and methods

2.1. Substrate and conversion coatings preparations

Aluminum alloy AA2024 and Magnesium alloy AZ31 (provided by Air Algérie Company, Algeria) were cleaned and pretreated for conversion coating. The samples having a surface area of 1 cm × 2.5 cm × 1 mm were grinded by SiC abrasive paper with grades from 100 to 1200, rinsed with absolute ethanol, quickly dried before immersion in the studied solution. For the coating evaluation, the samples were chemically treated in a solution containing 40 g / L of $\text{Na}_3\text{PO}_4 \cdot 12 \text{H}_2\text{O}$ at 60 °C, for 8 min, Then they were emerged in 200 ml of a solution of CH_3COOH and 50 g / L NaNO_3 , at room temperature, for 5 s. Samples were rinsed with distilled water after each step to remove contamination. The initial conversion bath containing 25 g / L of $(\text{Na}_2\text{MoO}_4 \cdot 2\text{H}_2\text{O})$ and 4 g / L NaF , with an adjustment of the PH to a value of 3.0, the temperature of 65 °C and we added 4g / l of cerium oxide to the molybdenum bath. The time emersion was optimized to 10 minutes.

2.2. Characterization techniques

The surface morphologies were observed through AFM (atomic force microscope) besides high-resolution SEM (scanning electronic microscope). The elemental composition was analyzed using EDAX (energy dispersive X-ray analysis). The Structural analysis of the Mo-CeO₂ coating obtained was achieved by means of X-ray apparatus (Bruker D8 Advance system) using $\text{CuK}\alpha$ monochromatic radiation ($\lambda = 0.15405 \text{ nm}$). the corrosion performance of conversion coating was characterized by Autolab potentiostat, the corrosive electrolyte was 3.5 g/l NaCl solution. Finally, the mechanical characterization was investigated by using Nano indentation (Anton Paar AE TTX) and The thickness measurement of the coatings was determined by an Elcometer brand coating thickness meter, based on the principle of magnetic induction.

3. Results and discussions:

3.1. Structural and Microstructural analysis

To see the morphology of the Mo-CeO₂ coating, we are using AFM (atomic force microscope). The 3D topographic images of the surface obtained by AFM measurements for Mo-CeO₂ coatings, scanned in the area of 500nm×500nm is presented in **Figure01**.

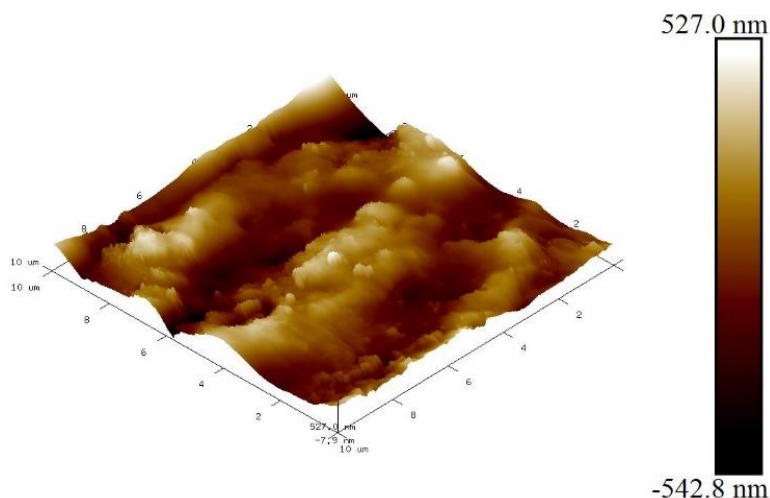


Figure 01: 3D topographic AFM images of Ni-SiO₂ nanocomposite coatings

Figure 2 shows the SEM coating morphological before the electrochemical tests. It is observed that the morphology of the Mo-CeO₂ coatings don't take the same format for the aluminum and magnesium alloys.

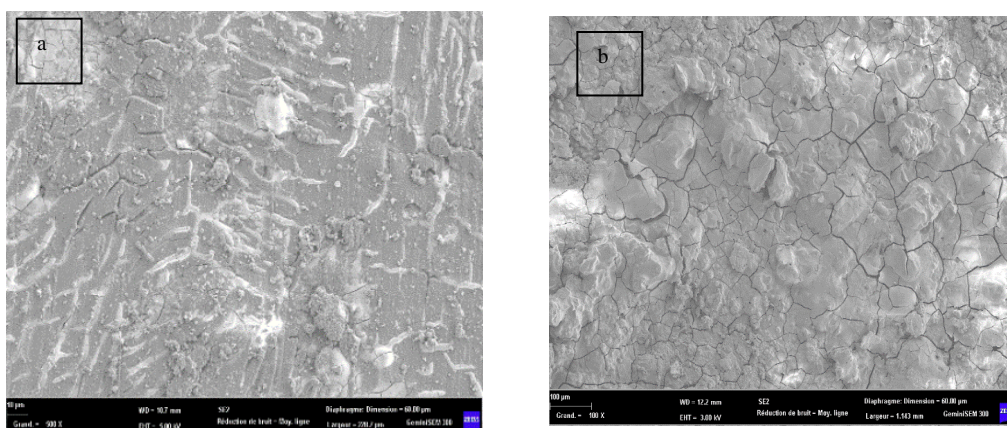


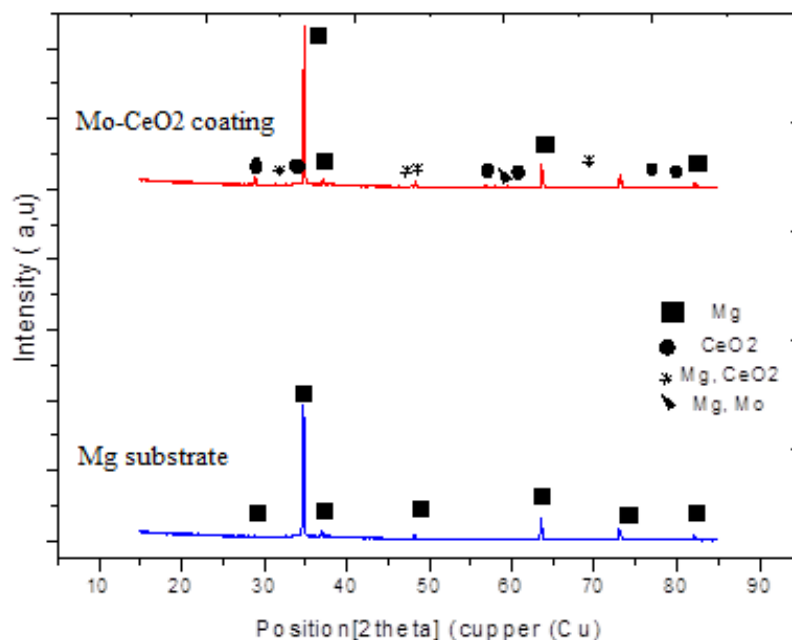
Figure 2: Morphology of the Mo CeO₂ coating on: a) aluminum substrate, b) magnesium substrate

For the aluminum substrate we can see a nanofiber of molybdenum was formed with uniform distribution of CeO₂ on the surface. In the case of magnesium substrate, we note the formation of small masses with an average size of non-uniform Mo and CeO₂ particles on all coatings. The coating formed in both substrates has pores, where their sizes are larger and larger near the interface, the more the micrograph shows a distribution of grains in the matrix based on aluminum or magnesium, the grains are different size, and there is a diffusion of grain towards the substrate. To confirm the nature of the chemical elements in each zone of the samples, X microanalyses were performed on the samples using the EDS technique. The following table shows the EDS analysis of samples. The results are summarized in table 1.

Table1: Mo-CeO₂ coating chemical composition

Aluminum substrate			Magnesium substrate		
Element	Weight %	Atomic %	Element	Weight %	Atomic %
C K	1.59	2.81	C K	4.13	5.93
O K	19.14	25.31	O K	62.39	67.32
F K	50.09	55.78	F K	27.07	24.60
NaK	13.82	12.72	NaK	1.83	1.38
MoL	15.36	3.39	MoL	3.62	0.65
CeL	0.87	0.09	CeL	0.96	0.12

The presence of Molybdenum, cerium and oxygen were confirmed in the surface of the both materials. The X-ray diffraction patterns obtained of the Mo-CeO₂ coating is presented in Figure 03. The peaks of XRD pattern have been assigned according to the JCPDS references CeO₂ (card No 9-062-1718) and Mo (card No 9-016-2278). Patterns of the as deposited films reveal the presence of cubic phase CeO₂ and cubic Mo with dominate peak for CeO₂ (111) and Mo (011) Moreover, apart these peaks there is only the substrate peak and the absence of any other peaks corresponding to impurities reveals the good quality of the deposited layers.

**Figure 3:** XRD patterns of Mo-CeO₂ conversion coating on Magnesium Alloy

3.2 corrosion behavior:

The Figure 4 presents the potentiodynamic polarization curves of the sample uncoated magnesium and aluminum substrates recorded after 2 h of immersion in 3.5% NaCl solution. Table 2 shows the summary of the electrochemical parameters obtained from these results. It appears clearly in Figure04 that the highest anodic and cathode densities were recorded for AZ31 and AL2024 in the NaCl solution in the absence of coating. The stabilization potential of

aluminum is however very close to its pitting potential. This behavior is related to the chemical attack of the chloride present in the corrosive solution [14,15]. The addition of cerium oxide into the coating in the NaCl medium leads to a decrease in corrosion current densities in the case of magnesium and offset the corrosion potential to more noble values. This observation is similar to the study of [16], who explained it by the inhibition effects of the Ce^{3+} ions. We see a sharp drop in corrosion speed and an improvement in corrosion resistance, which makes it possible to ensure on the effectiveness of the elaborate coating. The electrochemical spectroscopy impedance is carried out at an ambient temperature of 298k. Impedance diagrams were recorded at the corrosion potential, were illustrated on figure 05.

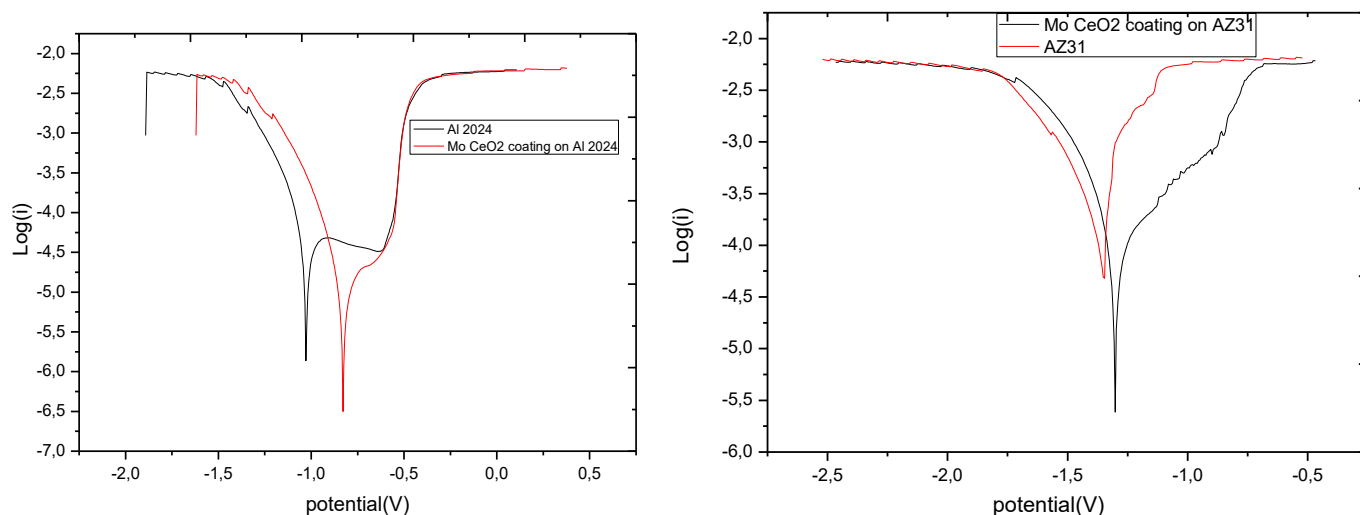


Figure 4 Potentiodynamic polarization curves obtained in NaCl 3.5 %

Table 2. Corrosion parameters determined from the Tafel plots

	-E(v)	I	B _c	B _a	R _p	V _{corr} (mm/y)
AL2024	1.0271	$3.8745 \cdot 10^{-5}$	0.47259	0.20404	1211.33	0.213
AL-Mo-Ce	0.82792	$5.3586 \cdot 10^{-6}$	0.13422	0.093199	552.323	0.08
AZ31	1.3488	0.0004901	0.30696	0.39366	108.203	1.0 58
AZ31-Mo-Ce	1.3022	0.0012498	0.31297	0.27706	115.931	0.55

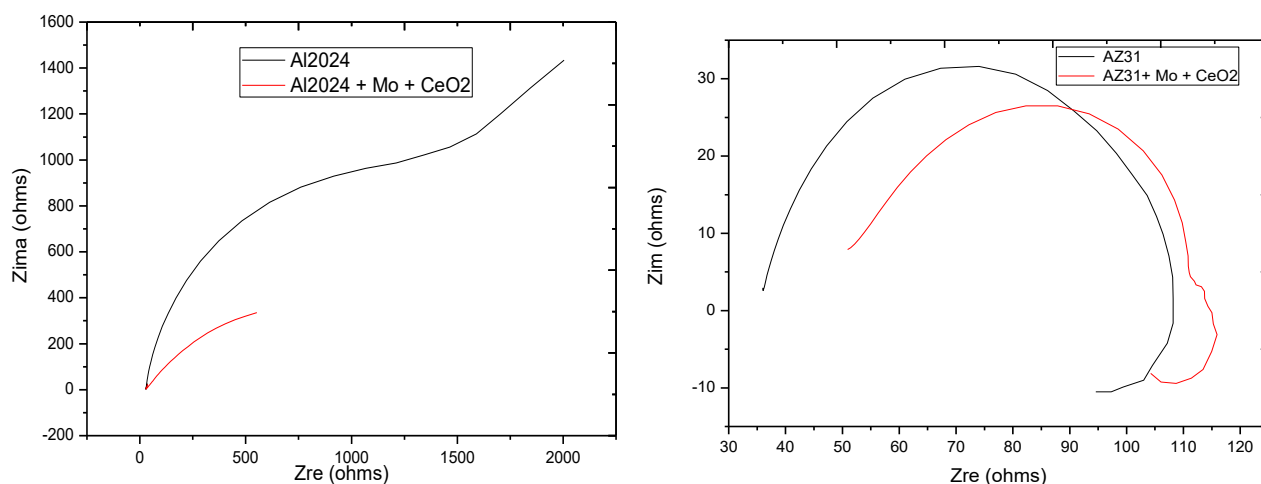


Figure 5: EIS Nyquist plots obtained for the Mo-CeO₂ coatings for the Al an Mg alloy

From the impedance diagrams made to the abandonment potential, we calculate the load transfer resistance (R_{tc}), the film resistance (R_f) and its capacity (C_f) and the capacity of the double Layer (C_{dl}) and therefore at the coating rates in the operating conditions used. The C values dl is calculated using the following equation and the values of the electrochemical parameters determined by the method of electrochemical impedance are presented in the table 3:

$$C_{dl} = \frac{1}{2 \times 3.14 \times R_f \times f_{max}}$$

Table 3: Corrosion impedance parameter for aluminum and magnesium alloys in the 3,5 % NaCl

.	Rt	Fmax	Cdl
AL	1211,33	0,398	0,00033029
AL-Mo-CeO ₂	552,323	0,1	0,00288302
Mg	108.203	79.433	1.85268 ^e -05
Ce Mo-CeO ₂	115.931	501.19	8.68248 ^E -09

From these results we notice that the response of the impedance is more stable in magnesium case than the case of aluminum. The substrate of aluminum presents phenomena of diffusion which can explain by destruction of passive film. However, the magnesium presents one capacitive boucle with bad corrosion resistance. The presence of the Mo-CeO₂ in the two materials increase in the capacity of the capacitive loop, characterizing the blocking of the charging transfer reaction, this film is increasingly resistant to the active dissolution of the metal [11].

3.3 Thickness measurement and, mechanical characterization

The table 04 presents the thickness measurements of the conversion coatings. It is observed that the thickness is not homogenous on the surface which is concordat with AFM results, for six measurements were done the thickness is more important in the case of magnesium substrate. The load-unload curves of the nano-indentation test performed in a force range of 20mN on Mo-CeO₂ coating at room is shown in Figure06. The elastic property and hardness of Mo-CeO₂ coating measured are respectively HV= 78.8 vickers and E_r = 34,898 GPa. The hardness of the coating is little elevate, it can give as a confirmation about the stability of the coating [6.10. 17].

Table4: Mo-CeO₂ coating thickness

Position	1	2	3	4	5	6	Average value (μ m)
AL2024+Mo-CeO ₂	3,7	5	4,6	8,7	8,1	3,6	5,61
AZ31+Mo-CeO ₂	33,3	23,7	25,6	39,7	32,9	33,3	31,41

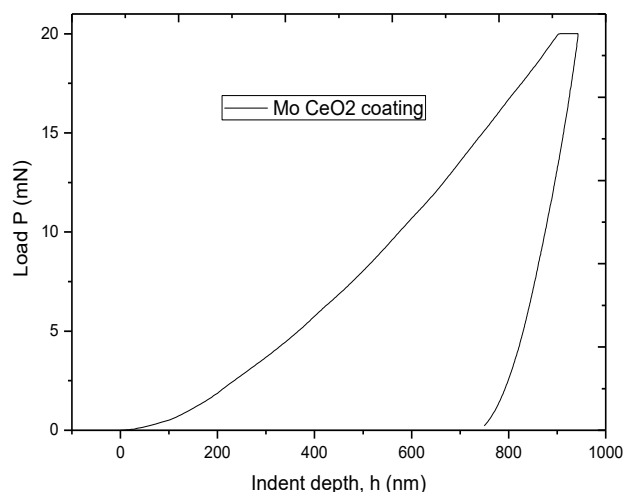


Figure 6: Load-unload curves of the nanoindentation test on Mo-CeO₂ coating at room temperature

4. Conclusion:

Mo-CeO₂ conversion coatings were formed on aluminum and magnesium substrates to improve mechanical and corrosion resistance. The morphology of the coating in all substrates was uniform with the presence of polycrystalline structure. Good mechanical proprieties were measured for the coating elaborated in term of hardness. The corrosion protection performance of the films was evaluated by, potentiodynamic polarization and EIS techniques. The results show that the presence of cerium oxide has significantly improved the corrosion protection properties of the Mo conversion coating. This effect is due to both increases in the barrier properties. This result is more significant in magnesium alloy.

5. References

- [1] J. Staley, D.L.-J.D.P. IV, undefined, Advances in Aluminum-Alloy Products Structural Applications in Transportation, (1993) (... ZI Court. AVE 7 AV).
- [2] A.Ziouche, M. Zergoug, N. Boucherrou, H. Boudjellal, M. Mokhtari, and S. Abaidia Pulsed Eddy Current Signal Analysis of Ferrous and Non-Ferrous Metals under Thermal and Corrosion Solicitations Russian Journal of Nondestructive Testing, 2017, Vol. 53, No. 9, pp. 652–659
- [3] Th. Lampke Dr.-Ing. , S. Darwich , B. Wielage , S. Steinhäuser Cost-efficient conversion coatings for corrosion protection prepared by the sol-gel process Materials science & engineering technology First published: 10 July 2008.
- [4] M. Terada, F.M. Queiroz, D.B.S. Aguiar, V.H. Ayusso, H. Costenaro, H.G. de Melo, I. Costa, M.-G. OlivierCorrosion resistance of tartaric-sulfuric acid anodized AA2024-T3 sealed with Ce and protected with hybrid sol–gel coating Surface & Coatings Technology 372 (2019) 422–426
- [5] Choukri Lekbir , Nessrine Dahoun , Asma Guetitech , Abdenour Hacid , Aicha ZIOUCHE , Kamel Ouaad , Amar Djadoun , Effect of Immersion Time and Cooling Mode on the Electrochemical Behavior of Hot-Dip Galvanized Steel in Sulfuric Acid Medium, Journal of Materials Engineering and Performance , Volume 26 , Issue 6 , 2017 , pp 2502-2511.
- [6] G.S. Chalakova, M.D. Datcheva, R.Z. Iankov, A.I. Baltov, D.S. Stoychev Comparative study via nanoindentation of the mechanical properties of conversion corrosion protective layers on aluminum formed in Cr⁶⁺-containing and Cr⁶⁺-free solutions Bulgarian Chemical Communications, Volume 48, Special Issue A, (pp. 64 - 70) 2016

- [7] Aliona Kirdeikiene, Olga Giršciene, Laima Gudavičiute, Vitalija Jasulaitiene, Algirdas Selskis, Skirmante Tutliene Self-Healing Properties of Cerium-Modified Molybdate Conversion Coating on Steel Journal reference: Coatings 2021, 11, 194.
- [8] C.I. Elsner, , A.R. Di Sarli C.R. Tomachuk Electrochemical Characterization of Chromate Free Conversion Coatings on Electrogalvanized Steel Materials Research. 2014; 17(1): 61-68 © 2014
- [9] K. Aggoun , L. Chaal, J. Creus, R. Sabot ; , B. Saidani, M. Jeannin Marine corrosion resistance of CeO₂/Mg(OH) mixed coating on a low alloyed steel Surface & Coatings Technology 372 (2019) 410–421
- [10] Fuxing Ye, Xu Sun Nanoindentation response analysis of TiN-Cu coating deposited by magnetron sputtering Progress in Natural Science: Materials International 28 (2018) 40–44.
- [11] M. Ostapiuk (2021) Corrosion resistance of PEO and primer coatings on magnesium alloy, Journal of Asian Ceramic Societies, 9:1, 40-52,
- [12] A.Ziouche, A. Haddad, R. Badji, M. Zergoug, N. Zoubiri, W. Bedjaoui, and S. Abaidia « Microstructure, Corrosion and Magnetic Behavior of an Aged Dual-Phase Stainless Steel” Journal of Materials Engineering and Performance, 2018; Volume 27, Issue 3, pp 1249–1256
- [13] X. Yu, G. Li, XPS study of cerium conversion coating on the anodized 2024 aluminum alloy J. Alloys Compd., 364 (1) (2004), pp. 193-198.
- [14] W.G. Fahrenholtz, et al. Characterization of cerium-based conversion coatings for corrosion protection of aluminum alloys Surf. Coat. Technol., 155 (2) (2002), pp. 208-213.
- [15] B. Hafez, M. Mokhtari, H. Elmsellem and H. Steli, Environmentally friendly inhibitor of the corrosion of mild steel: Commercial oil of Eucalyptus, Int. J. Corros. Scale Inhib., 2019, 8, no. 3, 573–585. doi: 10.17675/2305-6894-2019-8-3-8
- [16] C. Wang, S. Zhu, F. Jiang, F. Wang, Cerium conversion coatings for AZ91D magnesium alloy in ethanol solution and its corrosion resistance, Corros. Sci., 51 (2009), pp. 2916-2923, 10.1016/j.corsci.2009.08.003.
- [17] Attabi, S., Mokhtari, M., Taibi, Y. et al. J Bio Tribo Corros (2019) 5: 2. <https://doi.org/10.1007/s40735-018-0193-5>.
- [18] Corrosion inhibition potential of 2-[(5-methylpyrazol-3-yl)methyl]benzimidazole against carbon steel..., K. Chkirate, K. Azgaou, H. Elmsellem, et al., Journal of Molecular Liquids, 2021, 321, 114750 <https://doi.org/10.1016/j.molliq.2020.114750>
- [19] Anti-corrosion effect of Moroccan flax seeds oil as an eco-friendly inhibitor on mild steel in acidic media I. Najjari, A.M. Almehdi, F. Errachidi, Y. Kandri Rodi, M. Ramdani, I. Abdel-Rahman, F. Ouazzani Chahdi, I H. Steli, L. El Ghadraoui³ and H. Elmsellem Int. J. Corros. Scale Inhib., 2020, 9, no. 4, 1402–1418 doi: 10.17675/2305-6894-2020-9-4-13
- [20] A comparative study of two corrosion inhibitors: 1,4-diallyl-6-chloroquinoxaline 2,3-(1H,4H)-dione (1a) and 1,4-diallyl-6-nitroquinoxaline-2,3-(1H,4H)-dione (1b) A. El Janati, H. Elmsellem, Y. Kandri Rodi, Y. Ouzidan, M. Ramdani, M. Mokhtari, I. Abdel-Rahman, I. Cherif Alaoui, F. Ouazzani Chahdi and H.S. Kusuma Int. J. Corros. Scale Inhib., 2020, 9, no. 2, 644–660 644 doi: 10.17675/2305-6894-2020-9-2-17
- [21] Hicham Elmsellem, Yassir El Ouadi, Majda Mokhtari, Hajar Bendaif, Hanae Steli, Abdelouahed Aouniti, Ahmed M. Almehdi, Ibrahim Abdel-Rahman, Heri Septya Kusuma, Belkheir Hammouti. A NATURAL ANTIOXIDANT AND AN ENVIRONMENTALLY FRIENDLY INHIBITOR OF MILD STEEL CORROSION: A COMMERCIAL OIL OF BASIL (OCIMUM BASILICUM L.). Journal of Chemical Technology and Metallurgy. 4 (2019) 742-749.
- [22] H. Elmsellem, Nacer H., Halaimia F., Aouniti A., Lakehal I., Chetouani A., Al-Deyab S. S., Warad , R. Touzani, Hammouti B., Int. J. Electrochem. Sci. 9(2014)5328.